THERMAL STRUCTURE OF A MEGADIVERSE ANDEAN MOUNTAIN ECOSYSTEM IN SOUTHERN ECUADOR AND ITS REGIONALIZATION

Andreas Fries, Rütger Rollenbeck, Dietrich Göttlicher, Thomas Nauss, Jürgen Homeier, Thorsten Peters and Jörg Bendix

With 8 figures, 1 table, 3 photos and 1 supplement
Received 24 June 2009 · Accepted 20 November 2009

Summary: The thermal structure of a megadiverse mountain ecosystem in southern Ecuador is examined on the basis of temperature measurements inside the natural mountain forest and at open-sites along an altitudinal gradient from 1600 to 3200 m. The main methodological aim of the current study is to develop an air temperature regionalization tool to provide spatial datasets on average monthly mean, minimum and maximum temperature by using observation data. The maps, based on data of the period 1999–2007, are needed by ecological projects working on various plots where no climate station data are available. The temperature maps are generated by combining a straightforward detrending technique with a Digital Elevation Model and a satellite-based land cover classification which also provides the relative forest cover per pixel. The topical aim of the study is to investigate the thermal structure of both manifestations of our ecosystem (pastures and natural vegetation) with special considerations to the ecosystem temperature regulation service by converting natural forest into pasture. The results reveal a clear thermal differentiation over the year, partly triggered by the change of synoptic weather situation but also by land cover effects. Thermal amplitudes are particularly low during the main rainy season when cloudiness and air humidity are high, but markedly pronounced in the relative dry season when daily irradiance and outgoing nocturnal radiation cause distinct differences between the land cover units. Particularly the lower pasture areas gained by slash and burn of the natural forest exhibit the most extreme thermal conditions while the atmosphere inside the mountain forest is slightly cooler due to the regulating effects of the dense vegetation. Thus, clearing the forest clearly reduces the thermal regulation function (regulating ecosystem services) of the ecosystem which might become problematic under future global warming.

Zusammenfassung: Basierend auf Messdaten im Wald und auf offenen Flächen wird die thermische Struktur eines megadiversen Bergwaldökosystems in Süden Ecuadors entlang eine Höhengradienten von 1600 bis 3200 m untersucht. Das methodische Ziel der vorliegenden Arbeit ist die Entwicklung einer Regionalisierungsmethode für Lufttemperatur um flächendeckende Karten der mittleren monatlichen Minimum-, Mittel- und Maximumtemperatur bereitzustellen. Die Karten basieren auf Stationsdaten des Zeitraums 1999 bis 2007 und werden von ökologischen Projekten benötigt, auf deren Untersuchungsplots keine meteorologischen Messdaten verfügbar sind. Die Ableitung erfolgt mit einer einfachen Detrending Technik unter Hinzunahme eines Digitalen Geländemodells sowie einer aus Satellitenbildern abgeleiteten Landnutzungsklassifikation, die die relative Waldbedeckung pro Pixel beinhaltet. Es zeigen sich klare thermische Strukturen, die einerseits vom klimatischen Jahresgang, aber auch durch Unterschiede im Landbedeckungstyp hervorgerufen werden. Die thermische Amplitude entlang des Höhengradienten ist aufgrund hoher Bewölkung und Luftfeuchte kleiner in der relativen Regenzeit und besonders ausgeprägt in der relativen Trockenzeit, wenn die Strahlungsflüsse ungehindert einwirken können und die Unterschiede der Landnutzungsklassen klar hervortreten. Insbesondere die durch das Abbrennen des Naturwaldes im unteren Talbereich erzeugten Weideflächen zeigen die höchsten thermischen Extreme. Demgegenüber ist die Luft im Wald aufgrund der vielfältigen Regulations- und Schutzmöglichkeiten des dichten Kronenraums generell etwas kühler. Im Ergebnis bedeutet die Zerstörung von Bergregenwald eine Degradation der thermischen Regulationsfunktion des Gesamtökosystems (regulierende ökosystemare Dienstleistungen), was besonders im Hinblick auf den globalen Klimawandel problematisch erscheint.

Keywords: South Ecuador, air temperature, thermal structure, regionalization, forest and open land

1 Introduction

Globally biodiversity is threatened by land use changes including remote fertilization (especially nitrogen), and by the local effects of global climate change. Projections of biodiversity development by 2100 suggest that global warming is the dominating parameter affecting species composition in high mountain ecosystems (e.g. Sala et al. 2000; Thuiller 2007). This may also hold for the Andes of southern Ecuador which belongs to the five hottest hotspots of biodiversity, not only from the abundance of

vascular (Barthlott et al. 2007) and cryptogamic plants (Gradstein 2008). In the Ecuadorian Andes, a general warming trend is already observed in temperature data of the last decades and also indicated by the retreat of the ice caps of the Ecuadorian volcanoes (Bendix 2004; Vuille et al. 2008; Bendix et al. 2009). Particularly for ecothermic organisms, global warming and the rise of thermal altitudinal belts in high mountains could mean an area range shift with hitherto unknown consequences for species composition (e.g. Colwell et al. 2008; Bendix et al. 2009a). To test the present-day relation between organism groups and air temperature which is frequently the basis to estimate reactions of biodiversity on temperature changes by using so called envelope models (e.g. Thomas et al. 2004), reliable spatio-temporal information on air temperature must be available. However, climate data in mountain environments and particularly from tropical high mountains are hard to find (e.g. Barry 1992, 2008) and currently area-wide available global data fields which are frequently used in ecology, as e.g. the WorldClim database of Hijmans et al. (2005), reveal great uncertainties in regions like the tropical Andes of Ecuador (e.g. Sklenář et al. 2008). On the other hand, numerical models could also provide spatial fields of air temperature but the achievable accuracy at a model grid cell on the regional scale mainly depends on the selected cumulus parameterization scheme because of the strong coupling of cloud and rain formation and the radiation/thermal environment (Lynn et al. 2009).

A further challenge with regard to the plot-based studies of ecological research groups is the demand for very high resolution information on air temperature which is currently not provided by global circulation or mesoscale atmospheric models. Particularly in areas with complex terrain such as the Andes of Ecuador, model results have greater uncertainties because the topography is often not properly considered by the resolution of the model grid (e.g. Urrutia and Vuille 2009). Even if the spatial resolution of model results could be boosted by statistical downscaling techniques (Pape et al. 2009), the adaptation of the technique to produce high resolution temperature maps would require respective transfer functions for every pixel and thus, a spatial temperature field as an input (see e.g. Wilby et al. 2002).

One solution for the scaling problem could be the development and application of GIS-based energy balance models which have been proven to simulate air temperature with RMS accuracies of <1°C (e.g. Löffler and Pape 2004). A further challenge in providing temperature data to ecologists is the variability of the landscape because great areas of tropical mountain forests are currently converted to pasture land by slash and burn activities (for Ecuador refer to Hartig and Beck 2003) and thus, climate data must equally describe the thermal environment of different land cover units. By international standard, routine meteorological observations are normally available for open land (grass) where the thermal environment in adjacent forests can clearly differ (Bendix and Rafiqpoor 2001). If temperature observations are available, geostatistical interpolation techniques are generally powerful tools to provide the required high-resolution temperature maps (Pape et al. 2009). The availability of a digital elevation model and derived topographic variables like slope, aspect, altitude and geographical position could be integrated to improve the validity of climate maps (Wang et al. 2006; Daly et al. 2008). Overall, the most commonly used approach in meteorology for temperature regionalization is the kriging technique and its derivates (co-kriging, universal kriging, kriging with external drift KED) (e.g. Bendix and Bendix 1998; Vicente-Serrano et al. 2003). Goovaerts (2000) points out that no significant differences among the kriging derivates can be found. At the same time, kriging with detrended raw data offers more flexibility then kriging with external drift (Hudson and Wackernagel 1994), particularly when local trends such as the dependency between temperature and terrain elevation must be considered (Holdaway 1996). However, interpolation techniques are only successful if an appropriate dense coverage of climate stations in an area is given.

The present study is conducted in the framework of a multidisciplinary ecological research unit working in the Rio San Francisco valley of the eastern Andes of South Ecuador. Here, the ecologists require air temperature data to interpret their findings on e.g. species composition inside and outside the forest. However, air temperature is only observed at open-sites on a regular basis at meteorological stations, which are usually not located at the observation plots of the ecological groups.

The methodological aim of the study is to develop spatial temperature maps where the ecologists can extract average air temperatures for their observation plot, no matter if it is inside or outside the forest. We hypothesize that it is possible to derive high resolution temperature maps representing the thermal environment in- and outside the forest by combining long-term station data at open-sites, short-term temperature measurements inside the forest, a

satellite data based land cover classification encompassing information of relative forest cover per pixel, and a straightforward detrending technique.

The topical aim is to investigate the change of the thermal environment that occurs by converting natural forest into pasture, which can have severe impacts on e.g. species composition (see e.g. for bryophyts NÖSKE et al. 2008). We hypothesize that the thermal regulation function, one major ecosystem service, will be degraded by converting the natural forest to pasture land.

Moreover the calculated maps are the basis for the downscaling of future projections on air temperature derived from mesoscale model runs.

2 Study area and data

The area of the current study which is situated around the ECSF research station (Estación Científica de San Francisco, lat. 3°58'18" S, long. 79°4'45" W, alt. 1843 m a.s.l.) covers a part (~25 km^2) of the Rio San Francisco valley, deeply incised in the eastern cordillera of the South Ecuadorian Andes (Fig. 1). Elevations range from ~1600 m a.s.l. at the valley bottom to ~3200 m a.s.l. at the highest point, the Cerro del Consuelo. The natural vegetation is an evergreen forest covering the slopes from the valley bottom up to the tree line (~2700 m a.s.l.). With regard to the topographic position, the forest can

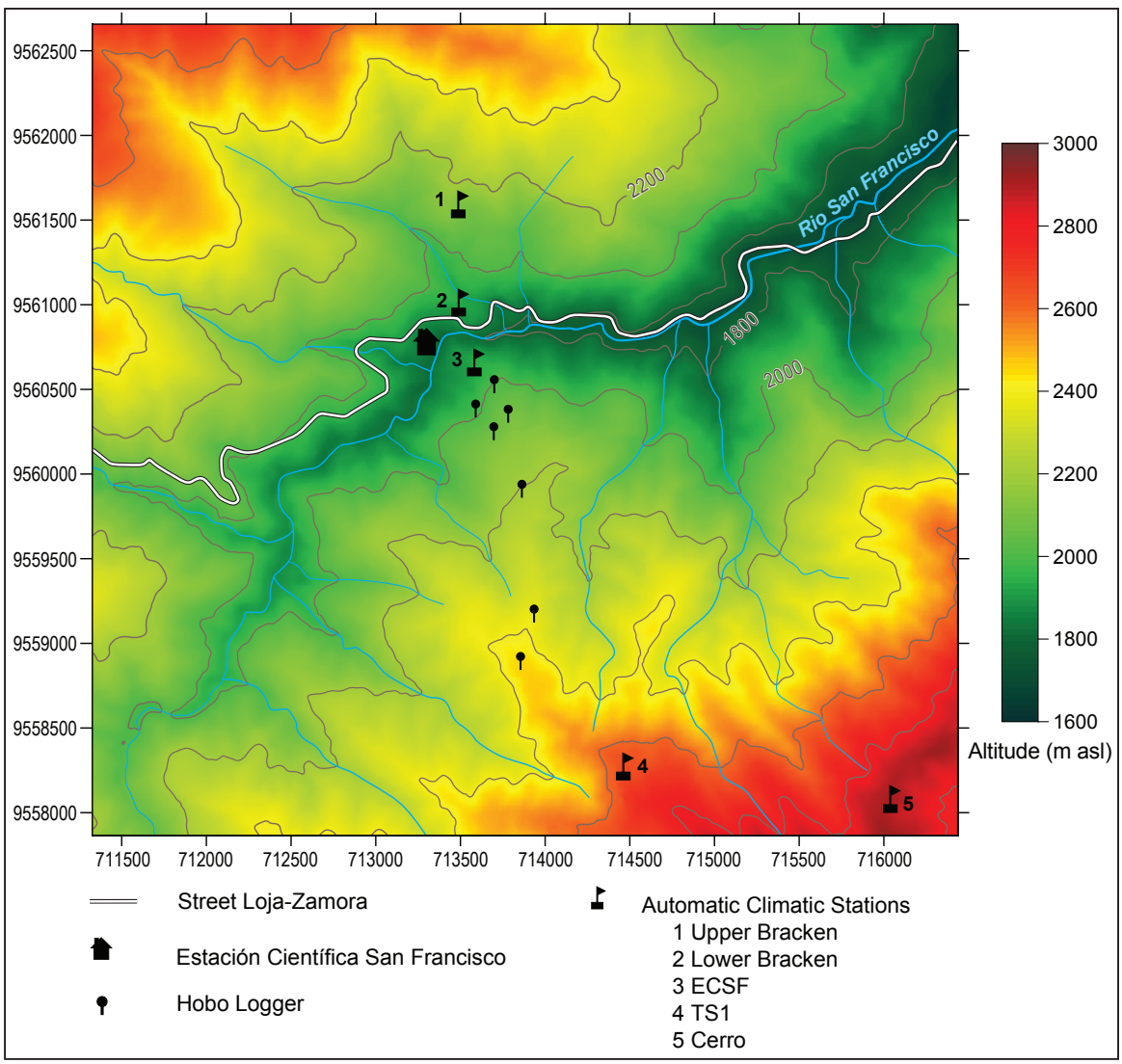

Fig. 1: Digital elevation model of the study area with meteorological stations and Hobo-Logger sites

be classified into evergreen lower montane forests (up to 2100–2200 m a.s.l.) and upper montane forests (2200–2700 m a.s.l.). Above ~2700 m a.s.l., a shrub-dominated sub-páramo prevails (Homeier et al. 2008). The reader may refer to Beck et al. (2008) for more detailed information on the study area. The climate of the area is perhumid with a marked elevational gradient in air temperature, cloudiness and rainfall (for details refer to Bendix et al. 2006a,b and 2008a,b,c). The basis data layer of the current study is a Digital Elevation Model (DEM) with a resolution of 10 x 10 m² per pixel (Fig. 1), which was originally derived from stereo aerial photos by aero-triangulation (Jordan et al. 2005).

For each pixel, land cover and the relative fraction of natural forest is derived from Landsat ETM+ satellite data (Fig. 2). Image processing encompasses topographic and atmospheric correction and the application of a soft classification algorithm using probability guided spectral unmixing (Göttlicher et al. 2009). The vegetation distribution map as well as the relative forest cover map is re-sampled to the resolution of the DEM (10 x 10 m²) using bilinear interpolation.

The left image in figure 2 illustrates that the forest of the south-facing slopes north of the Rio San Francisco has been cleared to gain pasture land, particularly in the lower parts of the valley where open land now dominates. Unfortunately, this important provisioning service for the local population (pasture use; see Knoke et al. 2009) has been degraded to a great extent due to the invasion of an aggressive weed, the southern bracken fern, which has led to the abandonment of many active pastures (see Hartig and Beck 2003). In the higher parts of the north-facing slopes, the natural forest changes into sub-páramo vegetation. The photos A-C below figure 2 demonstrate the three main land cover units: Forest, pasture and sub-páramo.

The right image in figure 2 illustrates the results of a soft land cover classification, representing the relative cover of forest in a 10 by 10 m² grid cell (Göttlicher et al. 2009). Reductions of relative cover in the forest at the north-facing slopes are generally due to natural landslides and the reduction of forest density in the transition zone towards the sub-páramo belt.

Climate observations were gathered in an operational network of five automatic climate stations at open-sites on the northern and southern slopes, and seven Hobo-Loggers (Onset Corp., USA) inside the forest on the southern slope (Fig. 1). Three automatic stations (ECSF: 1950 m a.s.l., TS1: 2669 m a.s.l., Cerro: 2933 m a.s.l.) have been operating since 1999 along an altitudinal gradient at the southern slope of the San Francisco valley. Two additional automatic stations were established on the northern slope of the valley (lower bracken in 2005: 1957 m a.s.l., upper bracken in 2007: 2113 m a.s.l.). The automatic stations measure the air temperature 2 m above ground as according to international standards. The near surface temperature at open-sites, which might also be important for organisms living close to the ground, generally shows higher amplitudes, but the daily course is also related to the air temperature. The seven Hobo-Loggers inside the natural forest of the north-facing slopes were operated from 2002 to 2005 along an altitudinal gradient from 1960 m a.s.l. to 2450 m a.s.l. Hobo-Loggers include sensors to measure air temperature and relative humidity. They were also mounted 2 m above the forest ground to maintain the same altitude as outside the forest to warrant comparability. However, due to the homogenous climate in the below canopy atmosphere, the observation height inside the forest is not as important as outside the forest due to the canopy shelter effect.

3 Method

Based on the information gained by the analysis of the observation data, the calculation of the spatial air temperature maps in 10 x 10 m² grid resolution is conducted by using a straightforward detrending technique.

The first step is the determination of average monthly lapse rates for all open-sites: the pasture area, the mountain forest and the shrub-dominated sub-páramo. The lapse rate is used to calculate the open-site air temperature with the following regression function:

$$T_{Month} = \Gamma \cdot z + b \qquad (1)$$

where T_{Month} is the average monthly air temperature [°C], Γ the slope (= the lapse rate), b the intercept of regression (the base level temperature) and z the altitude [m].

To consider the different locations of open-sites (pastures, forest and sub-páramo) properly, monthly maps are produced by applying three different lapse rates and base level temperatures (Tab. 1). In the lower part of the north-facing slopes (mountain forest) the lapse rate for open-sites between ECSF and TS1 is used (1999–2007). For the upper parts, mainly

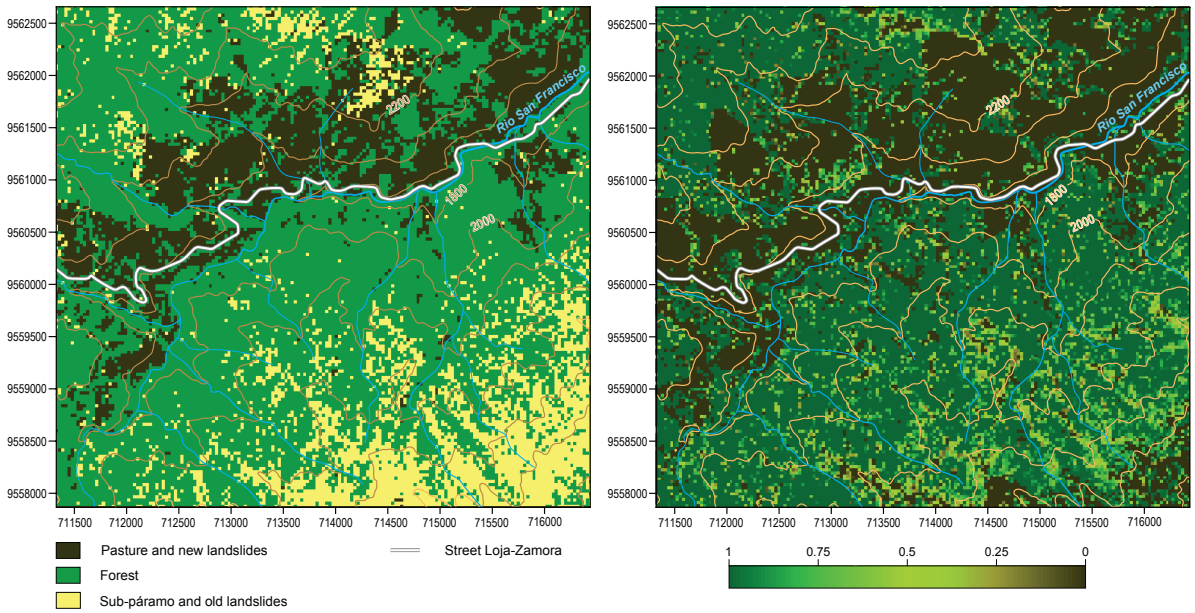

Fig. 2: (Left) Dominant land cover per pixel; (Right) Map of relative forest cover per pixel in the study area

Photo 1: Forest

Photo 2: Pasture

Photo 3: Sub-páramo

Table 1: Monthly average lapse rates (Γ) and base temperatures (b) at 0 m a.s.l. for mean, minimum and maximum air temperatures of the land use units.

	ECSF-TS1		TS1-Cerro		Pasture		Inside Forest	
Mean	Γ	**b**	Γ	**b**	Γ	**b**	Γ	**b**
Jan	-0.533	25.970	-0.640	28.837	-0.586	25.089	-0.302	21.604
Feb	-0.513	25.001	-0.611	30.163	-0.671	31.854	-0.371	22.469
Mar	-0.513	24.057	-0.698	37.183	-0.985	35.861	-0.431	22.771
Apr	-0.461	24.464	-0.773	32.720	-0.819	32.415	-0.443	22.678
May	-0.505	25.077	-0.696	30.109	-0.883	33.177	-0.461	23.272
Jun	-0.559	25.553	-0.530	24.760	-0.882	32.745	-0.378	22.286
Jul	-0.596	25.355	-0.392	22.247	-0.919	32.859	-0.304	21.489
Aug	-0.573	25.601	-0.644	27.211	-0.738	29.676	-0.282	20.726
Sep	-0.550	25.800	-0.698	32.469	-0.503	25.613	-0.350	22.446
Oct	-0.533	26.217	-0.698	30.348	-0.545	27.020	-0.312	21.645
Nov	-0.498	25.085	-0.726	34.286	-0.713	31.052	-0.337	21.887
Dec	-0.479	25.821	-0.733	30.762	-0.526	27.824	-0.363	22.488
Year	-0.526	25.970	-0.653	28.837	-0.731	30.432	-0.361	21.847
Max	**a**	**b**	**a**	**b**	**a**	**b**	**a**	**b**
Jan	-0.667	34.509	-0.952	40.604	-0.125	22.770	0.216	12.739
Feb	-0.460	29.959	-0.826	37.811	-0.243	24.816	0.339	11.832
Mar	-0.686	34.832	-0.950	40.213	-0.440	30.566	0.218	13.192
Apr	-0.695	34.668	-0.831	37.367	-0.318	27.624	0.133	14.824
May	-0.726	34.784	-0.916	38.854	-0.869	37.545	0.354	11.441
Jun	-0.492	28.894	-0.797	35.418	-0.399	27.311	0.068	16.031
Jul	-0.546	29.814	-0.802	35.134	-0.349	24.809	-0.112	18.816
Aug	-0.607	31.523	-0.858	36.621	-0.999	39.480	-0.138	18.917
Sep	-0.996	40.663	-1.052	42.034	-0.309	26.125	-0.169	20.286
Oct	-1.171	45.406	-1.158	44.978	0.120	19.220	0.074	16.486
Nov	-1.239	47.457	-1.193	46.560	-0.367	29.582	0.405	10.657
Dec	-1.047	42.490	-1.065	42.828	0.264	17.559	0.387	10.327
Year	-0.788	36.250	-0.950	39.868	-0.336	27.284	0.257	12.739
Min	**a**	**b**	**a**	**b**	**a**	**b**	**a**	**b**
Jan	-0.371	19.265	-0.359	19.038	-0.638	26.044	-0.520	24.277
Feb	-0.363	19.422	-0.380	19.851	-0.871	30.437	-0.469	22.322
Mar	-0.300	18.071	-0.359	19.445	-0.803	29.005	-0.495	23.522
Apr	-0.327	18.576	-0.362	19.499	-0.865	30.084	-0.510	23.943
May	-0.319	18.469	-0.372	19.645	-0.976	32.393	-0.502	23.841
Jun	-0.328	18.284	-0.367	19.205	-0.841	28.987	-0.510	23.844
Jul	-0.291	17.033	-0.339	18.267	-0.876	29.681	-0.535	23.393
Aug	-0.249	15.983	-0.329	17.919	-0.621	24.114	-0.534	23.120
Sep	-0.334	17.871	-0.352	18.362	-0.559	23.402	-0.535	22.956
Oct	-0.355	18.616	-0.359	18.906	-0.766	27.937	-0.492	22.485
Nov	-0.425	19.898	-0.338	18.077	-0.597	24.698	-0.494	23.238
Dec	-0.430	20.646	-0.385	19.834	-0.806	28.866	-0.454	22.097
Year	-0.338	18.443	-0.358	19.001	-0.768	27.971	-0.526	24.277

covered by sub-páramo vegetation, the lapse rate between TS1 and Cerro is applied. To derive a lapse rate for inside-forest plots and the pastures on the south-facing slopes, long-term open-site lapse rates are compared with the short-term lapse rates in the forest and on the pastures. Thus, the monthly relation of these short-term lapse rates to the long-term rates is determined (see figure 4). Then, the long-term open-site lapse rates are weighted with this relation so that comparable long-term lapse rates (representative for 1999–2007) are available also for inside-forest-sites and the pasture area which presupposes that relative differences between the land cover units are stationary over time. The next step is detrending to calculate the base level temperature of open-sites for the three land cover units (pasture, forest and sub-páramo) where the base level (A_{Det}) is set to 0 m a.s.l.

$$T_{Det} = T\text{-}\ (\Gamma \cdot (A_{Det} - A_{Station})) \qquad (2)$$

where T_{Det} [°C] is the average monthly base level 2 m air temperature of the land use unit, T [°C] the average monthly air temperature of the land use unit (1999-2007), Γ the monthly lapse rate of the land use unit [K m^{-1}], A_{Det} the detrending level [here 0 m a.s.l.] and $A_{Station}$ the altitude of the climate station [m a.s.l.].

The resulting base temperatures are merged with the DEM by inverting equation (2) and integrating the DEM. This step re-establishes the observed vertical distribution of air temperature for every grid/raster point. The inverted form of equation (2) can be written as:

$$T_{(x,y)} = T_{Det} + (\Gamma \cdot (A^{DEM}{}_{(x,y)} - A_{Det})) \quad (3)$$

where $T_{(x,y)}$ is the resulting monthly average air temperature [°C] at a grid cell position (x,y), T_{Det} the calculated detrended air temperature of the land units [°C], Γ the monthly lapse rate of the land use units [K m^{-1}], $A^{DEM}{}_{(x,y)}$ the altitude of the DEM grid cell at position (x,y) [m a.s.l.] and A_{Det} the detrending level [here 0 m a.s.l.].

The next step is to merge the three open-site air temperatures (pasture, forest, sub-páramo) with respect to the land cover classification. The respective temperatures are assigned to grid cells covered by pasture, forest and sub-páramo. The result is an open-site air temperature map representing all land cover classes.

Additionally, the lapse rate inside the forest stands is derived and regionalized in the same manner.

Finally, the real air temperature with regard of the relative forest cover per pixel is calculated by combining the open-site air temperature map with the inside-forest air temperature map. For every grid cell, the real air temperature is calculated as follows:

$$TLC_{(x,y)} = (T_{Forest} \cdot F_{Pro}) + (T_{Open} \cdot (1 - F_{Pro})) \qquad (4)$$

where $TLC_{(x,y)}$ is the land cover typ-weighted air temperature at position (x,y) [°C], T_{Forest} the calculated forest air temperature at position (x,y) [°C], F_{Pro} the relative proportion of forest (0-1) of a pixel at position (x,y) and T_{Open} the open land air temperature at position (x,y) [°C].

To produce also land cover type-weighted maps of average monthly minimum and maximum air temperatures, equations 1-4 are solved for monthly lapse rates and base temperatures of both thermal extremes (Tab. 1).

4 Thermal structure along the altitudinal gradient

The basis for temperature data regionalization using detrending is the analysis of the temperature lapse rate with terrain altitude, and its modification due to changes in land cover. Figure 3 shows the lapse rate for open-sites of the north-facing slopes.

The average monthly lapse rate for open-sites between ECSF and TS1 of the north-facing slopes generally reveals close to moist adiabatic conditions in the lower-mid altitudes (annual average lapse rate: -0.52 K/100 m), mainly due to high cloudiness and rainfall all year round (Bendix et al. 2006a,b). At the same time, the lapse rate in the sub-páramo region (TS1 to Cerro) shows a general tendency toward more dry adiabatic conditions, particularly in austral summer (annual average lapse rate: -0.70 K/100 m). Overall, the increased lapse rates at greater altitudes are due to the lower air temperature and reduced air density, causing lower vapor pressure. It is striking that the annual course of lapse rate development for both altitudinal belts is reversed in most months. The lapse rate in the upper part of the valley shows marked oscillation over the year and exceeds that of the lower parts particularly in austral winter (JJA). This can be explained by the humidity conditions in the valley. In the main rainy season of austral winter (June–August) cloud/fog frequency and thus air humidity is particularly high in the Cerro region which is frequently wrapped in cap clouds (Bendix et al. 2008c), espe-

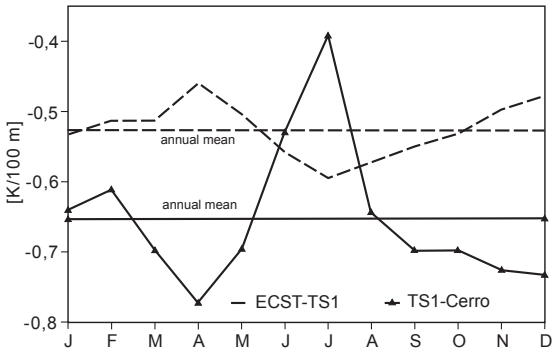

Fig. 3: Average monthly lapse rate at open-sites for the lower-mid and upper part of the north-facing slopes (1999–2007). For location of the stations refer to figure 1

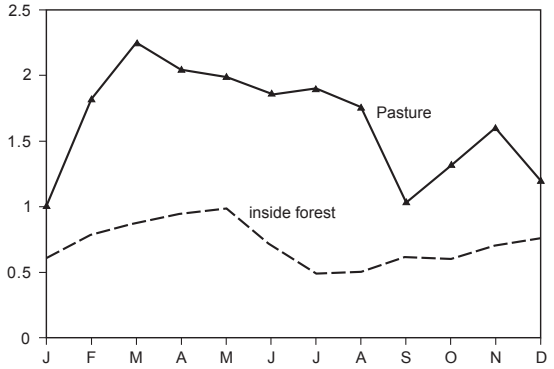

Fig. 4: Relative monthly lapse rate fraction of pasture and inside-forest with regard to the monthly lapse rate between ECSF-TS1 for the available time periods; 1 means the same lapse rate as for ECSF-TS1, <1 a lower (toward moist adiabatic) and >1 a higher (toward dry adiabatic) lapse rate

cially pronounced in June/July when the lapse rate in the highest parts clearly exceeds -0.6 K/100 m. At the same time, this period is characterized by a reduction of the lapse rate in the lower parts, which coincides with a slight decrease in fog frequency close to the valley bottom (Bendix et al. 2008c). In the relative dry season (September–May), cloudiness, fog frequency and thus, atmospheric moisture are clearly reduced in the Cerro region, leading to more dry adiabatic lapse rate conditions. At the same time, a reduced stratus frequency in the lower valley is slightly increased due to unhampered nocturnal radiation (Bendix et al. 2008c), leading to more moist adiabatic conditions. In summary, the lapse rate along the altitudinal gradient is not only a function of terrain altitude, but clearly linked to the atmospheric moisture dynamics.

The comparison of pasture and inside-forest lapse rates, indicated by the relative fraction in figure 4, shows that the atmosphere inside the mountain forest is characterized by more pronounced moist adiabatic conditions all year round. Particularly in July/August when the open-site lapse rate is reduced (Fig. 3), the gradient to the inside-forest lapse rate is increased, marked by a reduction of the relative fraction to ~0.5. The overall lower lapse rate all year round (relative fraction <1) means that adiabatic cooling with altitude is dampened inside the forest in comparison to open-sites. Assuming forest cover up to 3000 m a.s.l., a stationary lapse rate difference would result in a stronger cooling for open-sites from the valley bottom to the mountain top of about 2.4 K (1600–3000 m a.s.l.).

The contrary holds for the wide open areas of the pasture region on the south-facing slopes. Here, the lapse rate generally exceeds that of the north-facing slopes outside and inside the forest and thus, the lapse rate fraction is mostly >1.

The general reason for the difference between outside- and inside-forest-sites is the diverging atmospheric moisture condition. Figure 5 shows that average relative humidity inside the forest (p12) is always close to saturation compared to the open-sites (ECSF) where average humidity frequently falls below 90%, especially in the first half year. The shelter effect of the canopy against evaporative losses and the transpiration of the ample vegetation are the main reasons for the high humidity which prevents the establishment of more dry adiabatic lapse rates in the forest due to more frequent condensational heating. It is also depicted that humidity oscillations in the course of the year are clearly dampened inside the forest.

Of interest are not only lapse rate differences between open-sites and the below canopy atmosphere, but also the average monthly temperature differences which might be the result of a more direct/indirect exchange of daily ingoing and nocturnal outgoing radiation fluxes inside/outside the forest. Figure 6 illus-

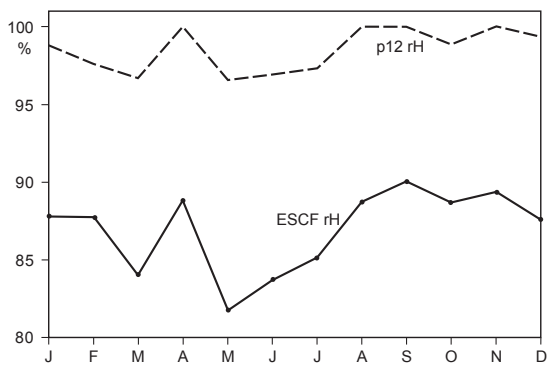

Fig. 5: Comparison of average monthly air humidity for an open-site (ECSF) and the Hobo-Logger site (p12) with a corresponding altitude, available years 2002–2003

trates that the forest is cooler in almost all months of the years 2002–2003. Only under specific conditions, the forest can be warmer than the open-site as indicated for January to April.

The reason might be a different course of cloudiness and thus irradiance. Figure 7 presents two typical days with (i) complete overcast and (ii) high solar irradiance.

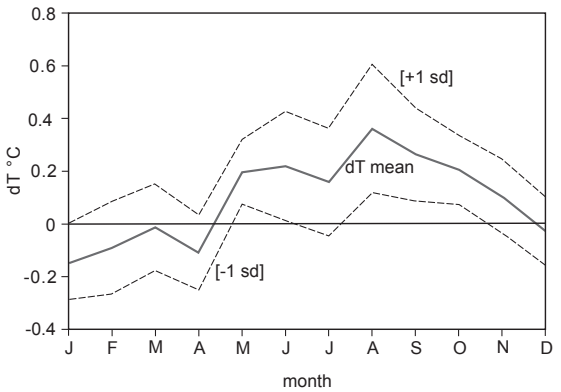

Fig. 6: Monthly air temperature difference and standard deviation between ECSF (open site) and the average reduced monthly temperature (reduction to ECSF met altitude of 1960 m a.s.l.) of inside-forest observations (7 plots; lapse rate for reduction is taken from figure 4), 2002–2003; sd = standard deviation

On cloudy days where radiation hardly exceeds 200 W m^{-2}, the forest-site is warmer almost all the time with a daily average of ~0.6°C. The opposite holds for sunny days where peak radiation exceeds 1000 W m^{-2}. Here, the forest is still warmer during the night, but clearly cooler during hours of high irradiance >200 W m^{-2}, which seems to be a threshold for a switch between positive and negative differences. This threshold is clearly exceeded on most days (see Bendix et al. 2008a), which means that the forest is generally colder on a daily average. This situation is illustrated for a sunny day where the forest is 0.3°C colder over the day than the adjacent open-site. Markedly, the thermal difference is mainly caused by daily irradiance. During night, the canopy shelters the inside-forest atmosphere from nocturnal radiation losses and mitigates the influence of cold air drainage flow due to forest roughness during all weather situations. During daylight however, cast shadow of the canopy and evaporative cooling are most likely factors which reduce heating rates inside the forest in comparison to the open-sites on the sunny day. On extremely overcast days, outgoing longwave radiation losses are more important in the radiation balance for the temperature development, which are reduced inside the forest due to the shelter effect of the canopy, thus causing slightly higher temperatures.

5 Spatial representation of air temperature in the San Francisco valley

Maps of averaged annual minimum, mean and maximum air temperature are presented in figure 8 and are representative for the observation period 1999–2007. The average air temperature ranges from 19.4 °C at the valley bottom to 9.4 °C at the upper parts. The lower parts of the north-facing slopes where great parts are covered by pastures are slightly warmer than the forest sites on the opposite side of the valley at the same altitudinal level. Particularly for the average annual minimum air temperature, the difference between the areas with different land cover types is clearly visible. As expected for the temperature minimum mostly occurring at the end of the night, the forest at corresponding altitudes

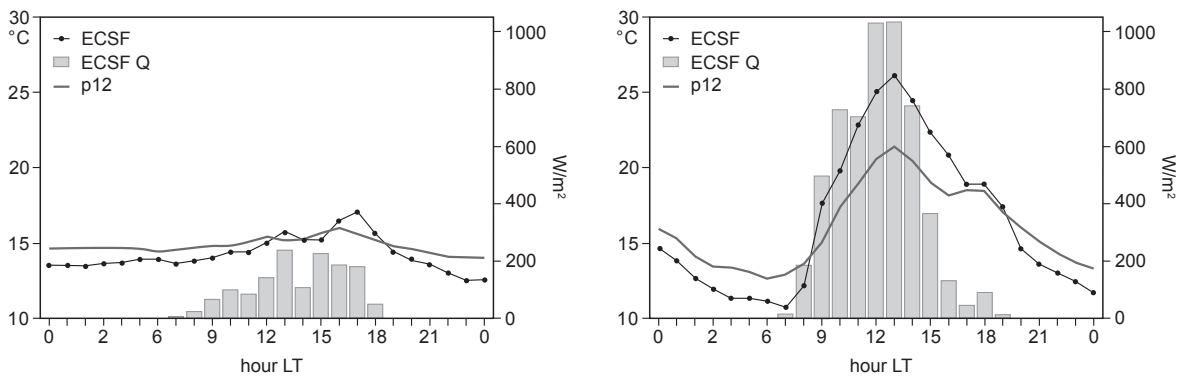

Fig. 7: Air temperature difference for an open-site (ECSF) and the Hobo-Logger site with a corresponding altitude (p12) and solar irradiance (Q) at (left) a typical cloudy (2 Jan 2003) and (right) sunny day (23 Jan 2003)

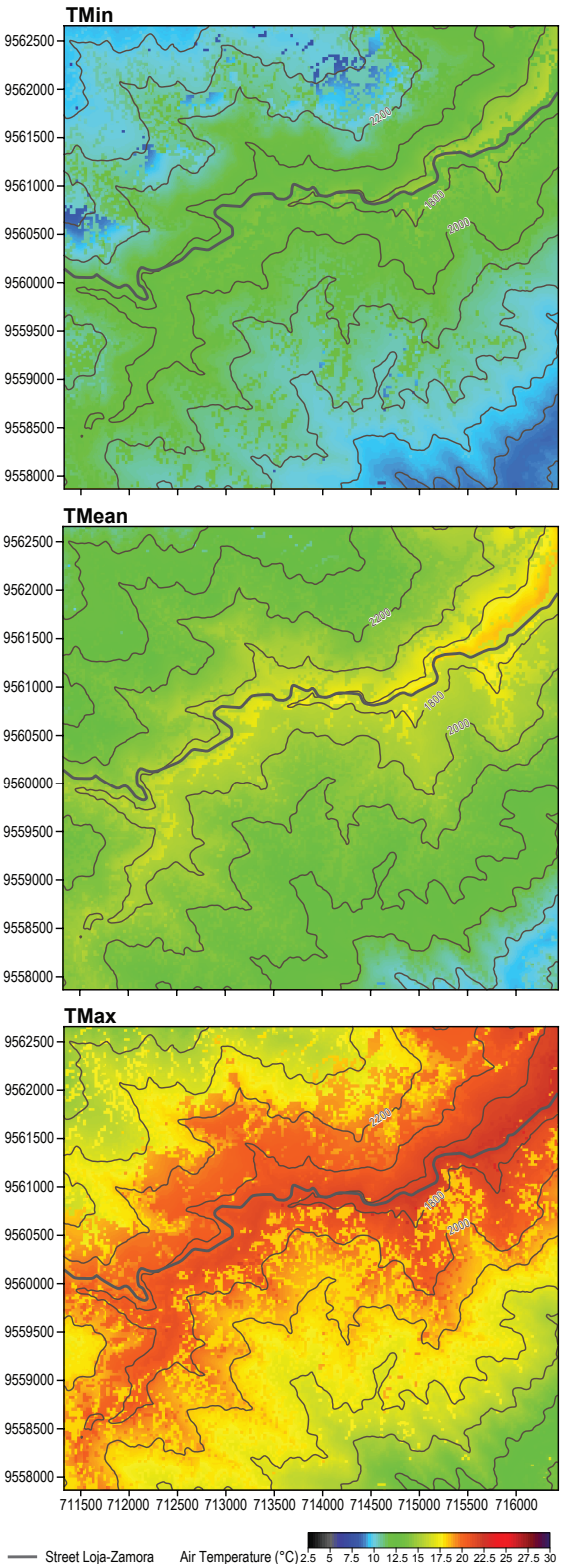

Fig. 8: Average annual 2 m minimum (TMin), mean (TMean) and maximum (TMax) air temperature in the study area

is warmer than the surrounding open-sites on both slopes. There is also a clear thermal difference between the open-sites. The lower pasture areas of the south-facing slopes are nearly as cold as the higher parts (sub-páramo) on the north-facing slopes. This is due to nocturnal cold air drainage flow particularly affecting the lower pastures while the higher parts of the north-facing slopes are more frequently protected against strong radiative cooling by the frequently occurring cap clouds, additionally providing condensation heating. Altogether, the average annual minimum air temperature ranges from ~15°C at the valley bottom to a minimum of ~5.8 °C at the lower pasture areas. The average annual maximum temperature ranges from ~26.2 °C at the valley bottom to ~10.8 °C in the upper parts. It is clearly visible that the areas which are exposed unsheltered to incoming solar radiation reach significantly higher maximum air temperatures than the below-canopy atmosphere in the forest. Particularly, the lower-level pasture-sites are affected by an exceptionally high temperature maximum in the respective altitudinal. This means that the average diurnal temperature amplitude is greatest on the lower pasture areas of the south-facing slopes while the lowest gradient occurs inside the natural forest of the north-facing slopes.

In the monthly average air temperature, the thermal differences between the three land cover units are generally maintained (see: supplement). However, the gradients slightly differ in the course of the year. Particularly in the main rainy season (June–August) when only little irradiance is available at the higher parts of the study area, lowest average temperatures occur in the study area while highest temperatures over the whole altitudinal gradient are reached in the relative dry season at the end of the year (November–December).

Of ecological interest is the average monthly minimum temperature which exhibits clear differences between the main rainy and relative dry seasons (see: supplement). In the first half of the year and particularly in the main rainy season, lowest minimum temperatures are obtained for the forest but the cooling of the pastures remains moderate. This changes toward the relative dry season at the end of the year (September–December) where the pastures clearly reveal the lowest temperatures because less cloudiness in this period enhance outgoing radiation at night (Bendix et al. 2009b), triggering radiative cooling of unprotected open-sites, and the development of katabatic flows which particularly affect the open-sites at lower altitudes close to the valley bottom.

The monthly course of the thermal structure in the study area can be well demonstrated by inspecting the average monthly maximum air temperature (see: supplement). Overall, the lowest maximum temperatures occur during the main rainy season when cloud frequency is high and concurrently the sun has its lowest elevation angle. During this time, the maximum air temperature values range between ~10°C at the sub-pàramo and ~23°C at the lowest parts of the valley bottom. While the maximum thermal amplitude along the altitudinal gradient is generally lower in this period (especially June-August), it is markedly high in the relative dry season at the end of the year (November–December). The highest maximum temperatures are calculated for austral summer with values between 11.4°C at the sub-pàramo and 29.1°C at the lowest part of the valley bottom. With regard to the three land cover units, the open land areas generally show a more pronounced daily heating than the below-forest atmosphere all year long. The maximum temperature in the natural forest is clearly influenced by the percentage of forest cover in the pixel because this determines cast shadow effects on the below-canopy atmosphere. With regard to open-sites, the sub-páramo vegetation at the mountain ridge is colder due to its greater terrain altitude and the higher cloud frequency, damping solar irradiance even in the relative dry season. At the same time, the pasture-sites in the lower parts of the valley exhibit the highest heating rates, particularly in the relative dry season at the end of the year. In the main rainy season, the maximum temperature gradients between pasture and forest nearly disappear due to the high cloud frequency and the corresponding low daily irradiance.

6 Discussion and conclusion

The combination of land cover classification and detrending technique has proven to be a feasible method for calculating air temperature maps with a high spatial resolution of 10 x 10 m² for the study area, the Rio San Francisco valley in the eastern Andes of southern Ecuador. One novel feature is to use different lapse rates as the basis of detrending, depending on land cover conditions and relative forest cover distribution. In other studies, detrended interpolation techniques have been used with a constant lapse rate for larger areas (Dodson and Marks 1997; Kurtzman and Kadmon 1999). However, the application of a common vertical temperature gradient for the whole study area cannot depict the complex conditions occurring in tropical mountains with a strong influence of cloud cover and the interaction of topographical features, land cover type and solar radiation. If applied to our study area, a unified lapse rate brought large deviations from a plausible temperature range for the extreme elevations. Air temperatures up to 37 °C were calculated for the lowest parts (data not shown) which have never been observed in reality. Obviously, the employment of different gradients for the various types of land cover and topographic locations is necessary to depict the real thermal structure. Pape et al (2009) proposed the integration of additional topographic variables in their geostastistical approach. However, they had more climate stations available and their domain is much larger. Also the dense vegetation with high rates of evapotranspiration, its variations in roughness and the different albedos in this study are probably more important factors than topographic characteristics.

The main goal was to give realistic estimates for the ecologists working in the field, because normally only data from the nearest climate station is used. The integration of further variables controlling the climate is intended for future extensions of the regionalization.

Some of the topographic effects are visible in the resulting maps. For example, minimum temperature shows clear evidence of cold air drainage. Influences of the cloudiness can be seen in the minimum maps because it limits outgoing radiation during the night, while at daytime it lowers maximum temperatures by reducing incoming solar radiation.

The most important feature of the maps is the capability to show the differences caused by land cover type. The differences are not that pronounced for the mean temperature, reaching 1 °C to 1.5 °C. This is in the same range Morecroft et al. (1998) found for woodland in the UK (0.6 °C to 0.9 °C). During sunny conditions the difference can be up to 3 °C. The highest deviation of maximum average temperature of 14.8 °C between pasture and forest is impressive and shows that forest stands are capable of maintaining much more homogeneous climate conditions, thus protecting sensitive organisms against climate extremes.

This extreme difference of maximum temperature was calculated for austral summer (NDJ), when solar radiation is pandering the south-facing slopes (pastures).

Although the dampening effect of dense forests has been shown by several studies (e.g. Grimmond et al. 2000; Körner and Paulsen 2004; Bader et

al 2006) this knowledge has hardly been used to produce temperature maps for ecological studies. Several processes interact, to enable this protective function: the canopy shelters the inside-forest atmosphere against high irradiance and nocturnal radiation losses. Evapo-transpirative cooling during day and condensation warming during night retain humidity in the forest always close to saturation and thus help to dampen temperature extremes. The high moisture content in the below-canopy atmosphere causes a reduction of the lapse rate and thus, a slower cooling with altitude. At last, the dense vegetation of the forest decelerates warm and cold advection (e.g. cold air drainage flow) due to the roughness of the ample biomass. All these balancing effects are absent for the lower level pastures and the high level sub-páramo area. Consequently, the conversion from natural forest to pasture degrades the thermal regulation function (supporting ecosystem services) of the ecosystem. The high thermal amplitudes also explain why reforestation of abandoned pastures with saplings of indigenous tree species sometimes show better results under the shelter of exotic tree plantations that protect the saplings from the climatic extremes of the open-pasture-sites (Weber et al. 2008). With regard to the annual course of weather in the study area, the clear difference between the rainy and the relative dry seasons is obvious. A high degree of cloudiness and rainfall throughout the day and the relatively low incoming and outgoing radiation fluxes obliterate the differences of air temperature between open land and inside-forest-sites, a situation typical for the rainy season in austral winter (JJA). On the other hand, pronounced radiative fluxes during the relative dry season clearly promote the strong thermal gradients between the different land cover types.

In the Páramo in Papallacta (close to the capital Quito) Bendix and Rafiqpoor (2001) found that soil temperature at -0.5 m is not constant during the year, because of the correlation between soil heat flux und air temperatures. If a strong gradient occurs between soil and atmosphere, a transfer of energy sets on. During the day this transfer is positive (orientated downward into the soil) and during the night negative (orientated upward to the soil surface and the atmosphere). This can be true for the different land cover parts in the study area, too. Körner (1998) points out that root growth (-0.1 m) starts at soil temperatures over 3 °C but does not reach sufficient intensity at temperatures less than 6 °C. Therefore root growth may be diminished during the night at the sub-páramo and the pasture areas at the south-facing slopes. Air temperature also controls the elevational limits of vegetation and plants distribution (Tang and Fang 2006). Hence, the low minimum air temperatures over the pastures can complicate reforestation and plant growth, especially during austral summer (NDJ) when the lowest air temperatures are calculated over the pastures areas. This initial study of regionalization has focused on longer-term averaged high resolution maps of air temperature, particularly useful for ecological applications. The methods will be enhanced to derive hourly maps, by using remote sensing data such as rain radar images (e.g. Rollenbeck and Bendix 2006) and satellite data products.

Acknowledgements

The authors are indebted to the German Research Foundation (DFG) for funding the study in the framework of the Research Unit FOR816. Meteorological data are provided by the projects RI 370/18-1, LE 762/10-1 and BE 1780/16-1, the analyses are conducted by project BE 1780/15-1. The authors also thank the foundation NCI for logistic support and the German Academic Exchange Service (DAAD) for a short-term funding of A. Fries.

References

Bader, M. Y.; Rietkerk, M. and Bregt, A. K. (2007): Vegetation structure and temperature regimes of tropical alpine treelines. In: Arctic, Antarctic, and Alpine Research 39 (3), 353–364.

Barry, R. G. (1992): Mountain climatology and past and potential future climatic changes in mountain regions: A review. In: Mount. Res. Develop. 12, 71–86. Doi:10.2307/3673749

– (2008): Mountain weather and climate. Cambridge.

Barry R. G. and Seimon A. (2000): Research for mountain area development: climatic fluctuations in the mountains of the Americas and their significance. In: Ambio 29 (7), 364–370.

Barthlott, W.; Hostert, A.; Kier, G.; Küper, W.; Kreft, H.; Mutke, J.; Rafiqpoor, M. D. and Sommer, J. H. (2007): Geographic patterns of vascular plant diversity at continental to global scales. In: Erdkunde 61, 305–315. Doi:10.3112/erdkunde.2007.04.01

Beck. E.; Makeschin, F.; Haubrich, F.; Richter, M.; Bendix, J. and Valarezo, C. (2008): Ecosystem (Reserva Biológica San Francisco). In: Beck, E.; Bendix, J.; Kottke, I.; Makeschin, F. and Mosandl, R (eds.) Gradients in

a tropical mountain ecosystem of Ecuador. Ecological Studies 198. Berlin, Heidelberg, 1–13.

Bendix, J. (2004): Extremereignisse und Klimavariabilität in den Anden von Ecuador und Peru. In: Geogr. Rdsch. 56, 10–16.

Bendix, J. and Bendix, A. (1998): Climatological aspects of the 1991/92 El Niño in Ecuador. In: Bulletin de L'Institut Francaise d'Etudes Andines 27, 655–666.

Bendix, J. and Rafiqpoor, M. D. (2001): Thermal conditions of soils in the Páramo of Papallacta (Ecuador) at the upper tree line. In: Erdkunde 55, 257–276. Doi:10.3112/erdkunde.2001.03.04

Bendix, J.; Rollenbeck, R.; Göttlicher, D. and Cermak, J. (2006a): Cloud occurrence and cloud properties in Ecuador. In: Clim. Research 30, 133-147. Doi:10.3354/cr030133

Bendix, J.; Rollenbeck, R. and Reudenbach, C. (2006b): Diurnal patterns of rainfall in a tropical Andean valley of southern Ecuador as seen by a vertically pointing K-band Doppler Radar. In: Int. J Climatol. 26, 829–847. Doi:10.1002/joc.1267

Bendix, J.; Rollenbeck, R.; Richter, M.; Fabian, P. and Emck, P. (2008a): Climate. In: Beck, E.; Bendix, J.; Kottke, I.; Makeschin, F. and Mosandl, R (eds.) Gradients in a tropical mountain ecosystem of Ecuador. Ecological Studies 198. Berlin, Heidelberg, 63–73.

Bendix, J.; Rollenbeck, R.; Fabian, P.; Emck, P.; Richter, M. and Beck, E. (2008b): Climate variability. In: Beck, E.; Bendix, J.; Kottke, I.; Makeschin, F. and Mosandl, R (eds.) Gradients in a tropical mountain ecosystem of Ecuador. Ecological Studies 198. Berlin, Heidelberg, 280-291.

Bendix, J.; Rollenbeck, R.; Göttlicher, D.; Nauss, T. and Fabian, P. (2008c): Seasonality and diurnal pattern of very low clouds in a deeply incised valley of the eastern tropical Andes (South Ecuador) as observed by a cost effective WebCam system. In: Meteorol. Appl. 15, 281–291.

Bendix, J.; Behling, H.; Peters, T; Richter, M. and Beck, E. (2009a): Functional biodiversity and climate change along an altitudinal gradient in a tropical mountain rainforest. In: Tscharntke, T.; Leuschner, C.; Veldkamp, E.; Faust, H.; Guhardja, E. and Bidin, A: (eds): Tropical rainforests and agroforests under global change. Berlin. (in press)

Bendix, J.; Trachte, K.; Cermak, J.; Rollenbeck, R. and Nauss, T. (2009b): Formation of convective clouds at the foothills of the tropical eastern Andes (South Ecuador). In: J. Appl. Meteorol. Climatol. 48. Doi:10.1175/2009JAMC2078.1

Colwell, R. K.; Brehm, G.; Cardelius, C. L.; Gilman, A. C. and Longino, J. T. (2008): Global warming, elevational range shifts, and lowland biotic attrition in the wet tropics. In: Science 322, 258–261. Doi:10.1126/science.1162547

Daly, C.; Halbleib, M.; Smith, J. I., Gibson, W. P.; Doggett, M. K., Taylor, G. H., Curtis, J. and Pasteris, P. P. (2008): Physiographically sensitive mapping of climatological temperature and precipitation across the conterminous United States. In: Int. J. Climatol. 28, 2031. Doi:10.1002/joc.1688

Dodson, R. and Marks, D. (1997): Daily air temperature interpolated at high spatial resolution over a large mountainous region. In: Clim. Research 8, 1–20. Doi:10.3354/cr008001

Göttlicher, D.; Obregón, A.; Homeier, J.; Rollenbeck, R.; Nauss, T. and Bendix, J. (2009): Land cover classification in the Andes of southern Ecuador using Landsat ETM+ data as a basis for SVAT modelling. In: Int. J. Remote Sens. 30, 1867–1886. Doi:10.1080/01431160802541531

Goovaerts, P. (2000): Geostatistical approaches for incorporating elevation into the spatial interpolation of rainfall. In: J. Hydrol. 228, 113–129. Doi:10.1016/S0022-1694(00)00144-X

Gradstein, S. R. (2008): Epiphytes of tropical montane forest – impact of deforestation and climate change. In: Biodiv. Ecol. Series 2, 51–65.

Grimmond, C. S. B.; Robeson, S. M and Schoof, J. T. (2000): Spatial variability of micro-climatic conditions within a mid-latitude deciduous forest. In Clim. Research 15, 137-149. Doi:10.3354/cr015137

Hartig, K. and Beck, E. (2003): The bracken fern (*Pteridium aquilinum*) dilemma in the Andes of South Ecuador. In: Ecotropica 9, 3–13.

Hijmans, R. J.; Cameron, S. E.; Parra, J. L.; Jones, P. G. and Jarvis, A. (2005): Very high resolution interpolated climate surfaces for global land areas. In: Int. J. Climatol. 25, 1965–1978. Doi:10.1002/joc.1276

Holdaway, M. R. (1996): Spatial modelling and interpolation of monthly temperature using kriging. In: Clim. Research 6, 215–225. Doi:10.3354/cr006215

Homeier, J.; Werner, F. A.; Gradstein, S. R.; Breckle, S.-W. and Richter, M. (2008): Potential vegetation and floristic composition of Andean forests in South Ecuador, with a focus on the RBSF. In: Beck, E.; Bendix, J.; Kottke, I.; Makeschin, F. and Mosandl, R (eds.) Gradients in a tropical mountain ecosystem of Ecuador. Ecological Studies 198. Berlin, Heidelberg, 87–100.

Hudson, G. and Wackernagel, H. (1994): Mapping temperature using Kriging with external drift: theory and an example from Scotland. In: Int. J. Climatol. 14, 77–91. Doi:10.1002/joc.3370140107

Jordan, E.; Ungerechts, L.; Cáceres, B.; Penafiel, A. and Francou, B. (2005): Estimation by photogrammetry of the glacier recession on the Cotopaxi Volcano (Ecuador) between 1956 and 1997. In: Hydrological Sciences 50, 949–961.

Knoke, T.; Weber, M.; Barkmann, J.; Pohle, P.; Calvas, B.; Medina, C.; Aguirre, N.; Günter, S.; Stimm, B.; Mosandl, R.; Walter, F. von; Maza, B. and Gerique, A. (2009): Effectiveness and distributional impacts of payments for reduced carbon emissions from deforestation. In: Erdkunde 63 (this issue), 365–384. Doi: 10.3112/erdkunde.2009.04.06

Körner, C. (1998): A re-assessment of high elevation tree line positions and their explanation. In: Oecologia 115, 445–459. Doi:10.1007/s004420050540

Körner, C. and Paulsen, J. (2004): A world-wide study of high altitude treeline temperatures. In: Journal of Biogeography 31 (5), 713–732.

Kurtzman, D. and Kadmon, R. (1999): Mapping of temperature variables in Israel: a comparison of different interpolation methods. In: Clim. Research 13, 33–43. Doi:10.3354/cr013033

Löffler, J. and Pape, R. (2004): Across scale temperature modelling using a simple approach for the characterisation of high mountain ecosystem complexity. In: Erdkunde 58, 331–348. Doi:10.3112/erdkunde.2004.04.04

Lynn, B. H.; Healy, R. and Druyan, L. M. (2009): Quantifying the sensitivity of simulated climate change to model configuration. In: Climatic Change 92, 275–298. Doi:10.1007/s10584-008-9494-x

Morecroft, M. D.; Taylor, M. E. and Oliver, H. R. (1998): Air and soil microclimates of deciduous woodland compared with an open site. In: Agric For Meteorol 90,141–156. Doi:10.1016/S0168-1923(97)00070-1

Nöske, N. M.; Hilt, N.; Werner, F. A.; Brehm, G.; Fiedler, K.; Sipman, H. and Gradstein, S. R. (2008): Disturbance effects on diversity of epiphytes and moths in a montane forest in Ecuador. In: Basic Appl. Ecology 9, 4–12. Doi:10.1016/j.baae.2007.06.014

Pape, R.; Wundram, D. and Löffler, J. (2009): Modelling near-surface temperature conditions in high mountain environments: an appraisal. In: Clim. Research 39, 99–109. Doi:10.3354/cr00795

Rollenbeck, R. and Bendix, J. (2006): Experimental calibration of a cost-effective X-band weather radar for climate ecological studies in southern Ecuador. In: Atmos. Research 79, 296–316. Doi:10.1016/j.atmosres.2005.06.005

Sala, O. E.; Chapin, F. S.; Armesto, J. J.; Berlow, E.; Bloomfield, J.; Dirzo, R.; Huber-Sanwald, E.; Huenneke, L. F.; Jackson, R. B.; Kinzig, A.; Leemans, R.; Lodge, D. M.; Mooney, H. A.; Oesterheld, M.; LeRoy Poff, N.; Sykes, M. T.; Walker, B. H.; Walker, M. and Wall, D. H. (2000): Global biodiversity scenarios for the year 2100. In: Science 287, 1770–1774. Doi:10.1126/science.287.5459.1770

Sklenář, P.; Bendix, J. and Balslev, H. (2008): Cloud frequency correlates to plant species composition in the high Andes of Ecuador. In: Basic Appl. Ecol. 9, 504–513. Doi:10.1016/j.baae.2007.09.007

Tang, Z. and Fang, J (2006): Temperature variation along the northern and southern slopes of Mt. Taibai, China. In: Agricultural and Forest Meteorology 139, 200–207.

Thomas, C. D.; Cameron, A.; Green, R. E.; Bakkenes, M.; Beaumont, L. J.; Collingham, Y. C.; Erasmus, B. F. N.; Ferreira de Siqueira, M.; Grainger, A.; Hannah, L.; Hughes, L.; Huntley, B.; van Jaarsveld, A. S.; Midgley, G. F., Miles, L.; Ortega-Huerta, M. A.; Peterson, A. T.; Phillips, O. L and Williams, S. E. (2004): Extinction risk from climate change. In: Nature 427, 145–148. Doi:10.1038/nature02121

Thuiller, W. (2007): Climate change and the ecologist. In: Nature 448, 550–552. Doi:10.1038/448550a

Urrutia, R. and Vuille, M. (2009): Climate change projections for tropical Andes using a regional climate model: temperature and precipitation simulations for the end of the 21st century. In: J. Geophys. Res. 114, D02108. Doi:10.1029/2008JD011021

Vicente-Serrano, S. M.; Saz-Sánchez, M. A and Cuadrat, J. M. (2003): Comparative analysis of interpolation methods in the middle Ebro Valley(Spain): application to annual precipitation and temperature. In: Clim. Research 24, 161–180. Doi:10.3354/cr024161

Vuille, M.; Francou, B.; Wagnon, P.; Juen, I.; Kaser, G.; Mark, B. G. and Bradley, R. S. (2008): Climate change and tropical Andean glaciers: past, present and future. In: Earth. Sci. Rev. 89, 479–496. Doi:10.1016/j.earscirev.2008.04.002

Wang, T.; Hamann, A.; Splittlehouse, D. L. and Aitken, S. N. (2006): Development of scale-free climate data for western Canada for use in resource management. In: Int. J. Climatol. 26, 383-397. Doi:10.1002/joc.1247

Weber, M.; Günter, S.; Aguirre, N.; Stimm, B. and Mosandl, R. (2008): Reforestation of abandoned pastures: silvicultural means to accelerate forest recovery and biodiversity. In: Beck, E.; Bendix, J.; Kottke, I.; Makeschin, F. and Mosandl, R (eds.) Gradients in a tropical mountain ecosystem of Ecuador. Ecological Studies 198. Berlin, Heidelberg, 431–441.

Wilby, R. L.; Dawson, C. W. and Barrow, E. M. (2002): SDSM - a decision support tool for the assessment of regional climate change impacts. In: Environ. and Modelling Software 17, 145-157. Doi:10.1016/S1364-8152(01)00060-3

Authors

Dipl.-Geogr. Andreas Fries
Dr. Rütger Rollenbeck
Dipl.-Geogr. Dietrich Göttlicher
Prof. Dr. Jörg Bendix
University of Marburg
Department of Geography
Deutschhausstr. 10
35032 Marburg
bendix@staff.uni-marbug.de
ruetger@web.de
dietrich.goettlicher@staff.uni-marburg.de
andy_fries@gmx.de

Prof. Dr. Thomas Nauß
University of Bayreuth
Faculty for Biology, Chemistry and Geosciences
Climatology Working Group
95440 Bayreuth
Thomas.Nauss@uni-bayreuth.de

Dr. Thorsten Peters
University Erlangen
Department of Geography
Kochstr. 4/4
91054 Erlangen
tpeters@geographie.uni-erlangen.de

Dr. Jürgen Homeier
Georg-August University Göttingen
Albrecht-von-Haller Institute of Plant Sciences
Grisebachstr. 1
Plant Ecology
37077 Göttingen
jhomeie@gwdg.de

Average monthly 2 m minimum (TMin), mean (TMean) and maximum (TMax) air temperatures in the study area